The Backscattering Factor for Systems with Non-uniform In-depth Profile

A. Jablonski
Institute of Physical Chemistry, Polish Academy of Sciences, ul. Kasprzaka 44/52, 01-224 Warsaw, Poland
jablo@ichf.edu.pl

(Received: January 2, 2009; Accepted: February 17, 2009)

It has been shown, in recent reports, that the backscattering factor (BF) in AES noticeably depends on the in-depth structure of the surface region. Consequently, the signal intensity due to an analyzed element in sputter depth profiling experiments cannot be described with a single BF value. The BF depends on the removed amount of the material and thus varies with time of sputtering. This effect is illustrated here on the example of the thin Ni layer buried in the Au matrix at different depths. The algorithms for calculating the BF for a thin layer of analyzed material are briefly discussed.

1. Introduction

We observe at present a renewed interest in determination of the backscattering factor (BF) for AES quantitative analysis. This term has been introduced into formalism of AES forty years ago [1]. In the early years of quantification of AES, much work has been devoted to establish a reliable source of this parameter. The frequently used source has been published by Shimizu and Ichimura [1,2] and Shimizu [3]. In recent years, a renewed interest in determination of the BF is observed due to several reasons. Firstly, in modern spectrometers the primary beam energies exceed considerably the limit of 10 keV assumed in Shimizu and Ichimura calculations [1-3], thus the data for higher energies are needed. Secondly, much progress has been made in calculations of the parameters necessary for calculations of the BF. One should mention here new sources of the differential elastic scattering cross sections [4-7] and the stopping power [8-10]. Finally, the usually used definition of the BF has been proved to be oversimplified in certain analytical conditions, and a new definition has been proposed [11-14].

The published sources of the BF values [1-3,11-14] contain data determined under assumption that the analyzed element is distributed uniformly in the region sampled by the AES analysis. However, we can expect that the non-uniform structure of the surface region may affect the energy and angular distribution of electrons at different depths in the surface region, and this distribution may be different from the distribution of electrons leaving the solid. Consequently, the BF value may depend on the sample structure. This problem is of importance in the AES sputter depth profiling experiments, and has been addressed in several recent works [15-18].

In the present work, several issues associated with the electron backscattering effects are approached. At first, we discuss the problem of further generalization of the BF definition. Secondly, brief overview of the relevant computational algorithms will be given. Finally, the case study of the buried layer in a uniform matrix material will be presented.

2. Definition of the backscattering factor

The Auger electron signal intensity, I_A, is typically expressed by

$$I_A = \frac{\Delta\Omega}{4\pi} T\, D\, I_0\, P_A\, \sigma_i(E_0) \sec\theta_0\, r\, N\, \lambda_{in} \cos\alpha \qquad (1)$$

where $\Delta\Omega$ is the solid acceptance angle of the analyzer, T is the analyzer transmission function, D is the detector efficiency, I_0 is the current of primary electrons, P_A is the probability that Auger transition follows the ionization, $\sigma_i(E_0)$ is the ionization cross section at the electron energy E_0, θ_0 is the incidence angle of the primary beam, r is the BF, N is the atomic density (i.e. the number of analyzed atoms per unit volume), λ_{in} is the Auger electron inelastic mean free path, and α is the emission angle of Auger electrons. The BF, r, corrects the signal intensity for ionizations due to backscattered electrons. The general expression defining this correction has the following form [11]

$$r = \int_0^\infty \Phi^*(z, E_0, \theta_0)\, \phi^*(\alpha, z)\, dz \qquad (2)$$

where $\Phi^*(z, E_0, \theta_0)$ is the excitation depth distribution function (EXDDF) and $\phi^*(\alpha, z)$ is the emission depth distribution function (EMDDF). First of these functions describes the density of ionizations as a function of depth, while the second function describes the probability that an Auger electron emitted at the depth z will reach the analyzer without energy loss [19]. The star superscripts indicate that both functions require a well defined normalization. The EXDDF is normalized as a ratio of the number of ionizations in a given layer inside a solid to the number of ionizations in the isolated layer. The EMDDF is normalized so that the integral with respect to depth is equal to unity.

It has been show that the general equation, under certain simplifying assumptions, can be transformed into a typically used formula [11]

$$r = 1 + \frac{\cos\theta_0}{I_0 \sigma_i(E_0)} \int_{E_c}^{E_0} \int_0^{\pi/2} I_B(E, \alpha_{in})\, \sigma_i(E) \sec\alpha_{in}\, d\alpha_{in}\, dE \tag{3}$$

where $I_B(E, \alpha)$ is the energy and angular distribution of electrons leaving the analyzed solid, E_c is the ionization energy, and α_{in} denotes the emission angle of inelastically backscattered electrons. This equation is frequently further simplified by assuming that the energy distribution and the emission angle distribution are independent, and the latter distribution is described by the cosine distribution.

$$I_B(E, \alpha_{in}) = I_B(E)\, g(\alpha_{in}) \tag{4}$$

$$g(\alpha_{in}) = 2 \sin\alpha_{in} \cos\alpha_{in} \tag{5}$$

Introducing Eqs (4) and (5) into Eq. (3), we obtain

$$r = 1 + \frac{2}{I_0 \sigma_i(E_0)} \int_{E_c}^{E_0} I_B(E)\, \sigma_i(E)\, dE \tag{6}$$

Let us consider a simple model of a non-uniform solid in which we analyze a thin layer of a given element of thickness Δt located at a depth t in a certain matrix element (Fig. 1). As an example, we analyze here the case of the Ni layer in the Au matrix. The general definition of the BF [Eq. (2)] can be readily modified for calculating this parameter for a buried layer. Zommer and Jablonski [17] proposed the following defining formula for such a case

$$r = \int_t^{t+\Delta t} \Phi^*(z, E_0, \theta_0)\, \phi^*(\alpha, z)\, dz \tag{7}$$

where now we normalize the EMDDF, $\phi(\alpha, z)$, according to the formula

$$\phi^*(\alpha, z) = \frac{\phi(\alpha, z)}{\int_t^{t+\Delta t} \phi(\alpha, z)\, dz} \tag{8}$$

Suppose that the layer thickness is so small that the electron trajectories in the depth sampled by AES are practically identical with the trajectories in the same region in a pure matrix material. We can prove that, if the thickness Δt approaches zero, the BF calculated from Eqs (7) and (8) approaches the EXDDF value for a given depth

$$r \to r(t) \cong \Phi^*(t, E_0, \theta_0) \tag{9}$$

In the present work, we compare the BF values calculated from three defining formulas [Eqs (2), (3) and (9)].

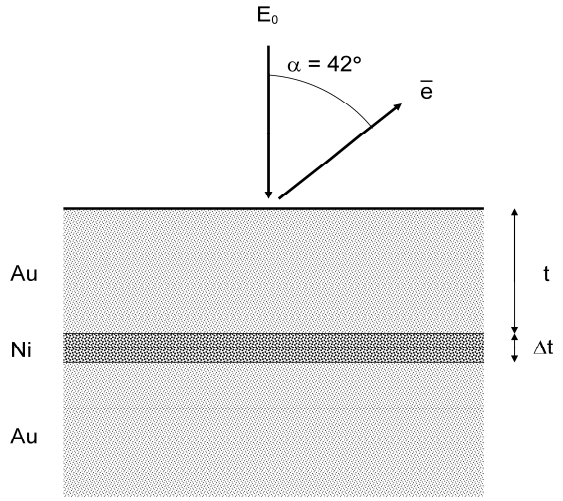

Fig. 1 Model of the solid and the experimental configuration considered in the present work.

3. Results and discussion

The BF originating from three definitions was evaluated from the Monte Carlo simulations of electron trajectories in a solid. The relevant algorithms implemented the continuous slowing down approximation (CSDA). The main input data are then the differential elastic scattering cross sections (DCS) to describe the elastic scattering events, and the stopping power (SP) to describe the

energy decrease along the trajectory length. Calculations were made for the Ni L_3VV Auger transition with kinetic energy of 846 eV. The DCSs were calculated from the program ELSEPA for energies ranging from the ionization energy of the Ni L_3 electron shell up to energy of 30 keV [6]. Calculations were made for 50 energies logarithmically distributed, and the cross sections during simulation were determined by interpolation. The stopping power was calculated from the recently published analytical function fitted to the SPs obtained from the optical data [10]

$$S = \frac{D\,E^{d_2^*}\ln(d_3^*\,E)}{\lambda_{in}} \tag{10}$$

where coefficients D, d_2^* and d_3^* are tabulated for 41 elemental solids [10]. The IMFP values for the Au matrix were calculated from the equation proposed by Tanuma et al. [20]. This equation has been found to be satisfactory for energies up to 30 keV [21]. Additionally, algorithms for calculating the BF need the ionization cross section for considered energy range. The expression of Casnati et al. [22] was used in the present calculations

The defining formula given by Eq. (3) does not distinguish between two cases: (i) the AuNi alloy with low concentration of Ni uniformly distributed in the surface region, and (ii) a thin Ni layer located at a certain depth. We expect that in both cases the angular and energy distribution of electrons leaving the solid would be very similar. Thus, calculations of the BF from Eq. (3) were performed here as a reference case. At first, the integrated angular distribution of electrons leaving the solid was calculated from the MC simulations

$$G(\alpha_{in}) = \int_{E_c}^{E_0} I_B(E,\alpha_{in})\,\sigma_i(E)\,dE \tag{11}$$

In the second stage, this distribution was integrated numerically

$$r = 1 + \frac{\cos\theta_0}{I_0\sigma_i(E_0)}\int_0^{\pi/2}\frac{G(\alpha_{in})}{\cos\alpha_{in}}\,d\alpha_{in} \tag{12}$$

Fig. 2 shows comparisons of the angular distribution $G(\alpha_{in})$ with the cosine distribution $g(\alpha_{in})$. We see that, in the wide range of energies, both distributions differ noticeably. A particularly pronounced difference is observed at the lowest energy considered, i.e. 2 keV. Thus, the simplifying approximations given by Eqs (4) and (5) are generally not valid, and should be avoided.

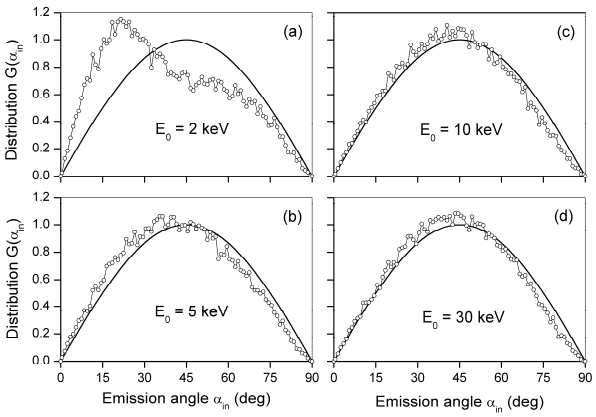

Fig. 2 The integrated angular distribution $G(\alpha_{in})$ [Eq. (11)] calculated for Ni L_3VV Auger electrons (circles). For comparison, the cosine distribution is also shown (solid line). (a) Primary energy equal to 2 keV; (b) 5 keV; (c) 10 keV; and (d) 30 keV.

The use of the generalized definition of the BF leads to different BF values for the uniform distribution of Ni in the matrix material, and for the buried layer. To check this, we need an algorithm for calculations of the EXDDF. The Monte Carlo strategy implementing the CSDA for calculating the EXDDF function has been recently published [14]. It consists in dividing the surface region into thin layers, and determining the number of ionizations for each layer. Interested reader is referred to the original work for details [14]. In this way, we calculate the depth dependence of the BF for the burried layer, $r(t)$ [Cf. Eq. (9)]. The BF a diluted Ni alloy should be calculated from Eq. (2). In that case, we also need the MC algorithm for calculations of the EMDDF. Details of algorithm used in present work were described in recent publications [23,24].

At first, the BF calculated from the general definition for uniform solids [Eq. (2)] was compared with BF calculated from the usually used definition [Eq. (3)]. Results of calculations are shown in Fig. 3(a). Additionally, the BFs resulting from the Shimizu formula [3] are shown there. We see, that both definitions lead to distinctly different BF values, particularly at energies close to the ionization energy. The percentage difference, shown in Fig. 3(c) reaches 10% in the range between 2 keV and 10 keV, and exhibits decreasing tendency at higher energies. We also see that the BFs resulting from the Shimizu formula deviate from the BFs calculated from Eq. (3). This is mainly due to the fact that different input parameters were used in calculations of Shimizu, and there were differences in the MC strategy.

Good agreement of the Shimizu BFs with the BFs calculated from the general definition is fortuitous.

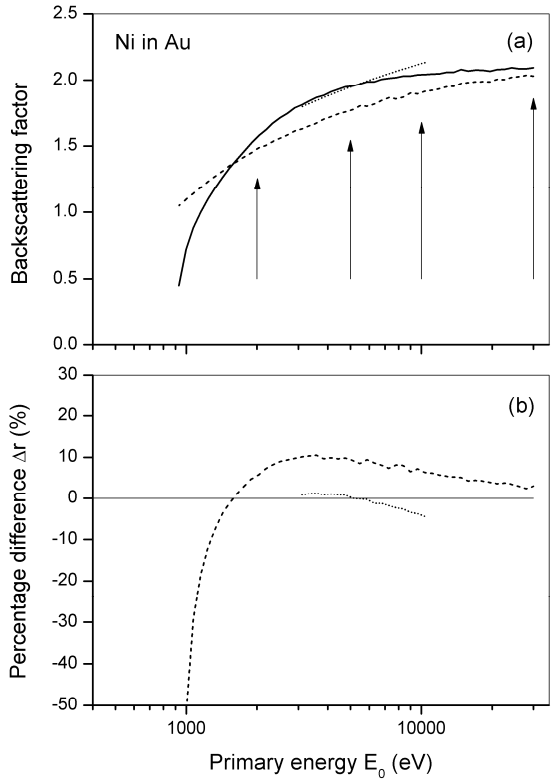

Fig. 3 (Upper panel) The BF calculated for the diluted Ni alloy in Au. Solid line: the general definition [Eq. (2)]; dashed line: BFs calculated from Eq. (3); dotted line: BFs calculated from the Shimizu formula. Arrows indicate energies considered here in calculation for the buried Ni layer. (Lower panel). The percentage differences with respect to the BFs calculated from the general definition. Dashed line: BFs calculated from Eq. (3); dotted line: BFs calculated from the Shimizu formula.

Arrows in Fig 3(a) indicate energies for which the depth dependence of the BF for the Ni layer was calculated. The results are shown in Fig. 4. We see that the BF calculated for the Ni layer dramatically varies with depth at which the layer is located. Furthermore, this dependence has a different shape for different energies. At 2 keV, the BF passes a maximum approximately at about 10 angstroms. For higher energies, the BF is decreasing with the decreasing depth. We note that the minimum BF value is observed for the layer located at the surface. This value is close to the BF calculated from the usual formula [Eq.(3)]. Such a result is expected since the energy and angular distribution of electrons leaving the solid is in that case very close to the distribution of electron inside this layer.

$$r(0) = \Phi^*(0, E_0, \theta_0) = 1 + \frac{\cos\theta_0}{I_0 \sigma_i(E_0)} \int_{E_c}^{E_0} \int_0^{\pi/2} I_B(E, \alpha_{in}) \sigma_i(E) \sec\alpha_{in} \, d\alpha_{in} \, dE \tag{13}$$

This result has been noticed earlier. The EXDDF is identical with the "Phi-Rho-Zi" function of electron probe microanalysis (EPMA). In several reports [25,26], the surface value of the "Phi-Rho-Zi" function has actually been recommended to use as the BF for AES.

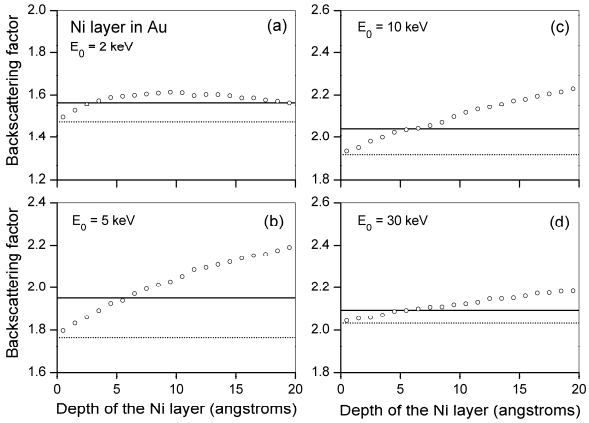

Fig. 4 The depth dependence of the BF for the Ni layer calculated from Eq. (9) (circles). For comparison, the BF calculated for uniform solid from Eq. (2) (solid line) and Eq. (3) (dotted line) are also shown here (a) Primary energy equal to 2 keV; (b) 5 keV; (c) 10 keV; and (d) 30 keV.

4. Conclusions

The depth dependence of the BF for a thin layer proves that the AES signal intensity depends on the structure of the solid. During the sputter depth profiling, the BF varies as the surface structure changes. The AES signal enhancement due to scattered electrons is then difficult to determine from a simple routine procedure. In general, as follows from Eq. (2), the BF depends on parameters defining the experimental configuration: primary energy, E_0, incidence angle, θ_0, and the emission angle α. In addition, the BF depends on the solid and the selected Auger transition: ionization energy, Auger electron energy, composition of the surface region, and finally, as discussed above, on the structure of the region sampled by Auger electrons. It would be rather difficult to derive an analytical

universal formula, similar to the Shimizu [3] formula, for the use in data processing in sputter depth profiling. On the other hand, calculations of the signal intensity for the multilayer structure have proved that the account for electron backscattering distinctly improves agreement between theory and experiment [18]. A possible solution would be the development of a user friendly dedicated software for simulating the AES signal intensity for layered systems. Such work is planned for the future.

5. References

[1] R. Shimizu and S. Ichimura, *Quantitative Analysis by Auger Electron Spectroscopy*, Toyota Foundation Research Report No. I-006 76-0175, Tokyo, 1981.
[2] S. Ichimura and R. Shimizu, Surf. Sci. **112**, 386 (1981).
[3] R. Shimizu, Jpn. J. Appl. Phys. **22**, 1631 (1983).
[4] A. Jablonski, F. Salvat, and C. J. Powell, NIST Electron Elastic-Scattering Cross-Section Database, Version 3.1, Standard Reference Data Program Database 64, U.S. Department of Commerce, National Institute of Standards and Technology, Gaithersburg, MD (2003); http://www.nist.gov/srd/nist64.htm
[5] A. Jablonski, F. Salvat and C. J. Powell, J. Phys. Chem. Ref. Data **33**, 409 (2004).
[6] F. Salvat, A. Jablonski and C. J. Powell, Comput. Phys. Commun. **165**, 157 (2005).
[7] *Elastic Scattering of Electrons and Positrons*, ICRU Report 77, Journal of ICRU Vol. 7., Oxford University Press, Oxford (2007); http://www.icru.org.
[8] S. Tanuma, C. J. Powell and D. R. Penn, Surface Interface Anal. **37**, 978 (2005).
[9] S. Tanuma, C. J. Powell and D. R. Penn, J. Appl. Phys. **103**, 063707 (2008).
[10] A. Jablonski, S. Tanuma and C. J. Powell, J. Appl. Phys. **103**, 063708 (2008).
[11] A. Jablonski, Surf. Sci. **499**, 219 (2002).
[12] A. Jablonski and C. J. Powell, Surface Sci. **574**, 219 (2005).
[13] Z. J. Deng, W. S. Tan and Y. G. Li, J. Appl. Phys. **99**, 084903 (2006).
[14] A. Jablonski and C. J. Powell, Surface Sci. **601**, 965 (2007).
[15] S. Hofmann and J. Y. Wang, Surface Interface Anal. **39**, 324 (2007).
[16] S. Hofmann, J. Y. Wang and A. Zalar, Surface Interface Anal. **39**, 787 (2007).
[17] L. Zommer and A. Jablonski, J. Phys. D, Appl. Phys. **41**, 055501 (2008).
[18] L. Zommer, A. Jablonski, L. Kotis and M. Menyhard, J. Phys. D, Appl. Phys. **41**, 055512 (2008).
[19] ASTM E673-03, Standard Terminology Relating to Surface Analysis, Annual Book of ASTM Standards 2006, Vol. 3.06, ASTM International, West Conshohocken, 2006, p. 647.
[20] S. Tanuma, C. J. Powell and D. R. Penn, Surf. Interface Anal. **17**, 911 (1991).
[21] S. Tanuma, private communication.
[22] E. Casnati, A. Tartari and C. Baraldi, J. Phys. B **15**, 155 (1982).
[23] A. Jablonski and C. J. Powell, Surface Sci. 520, 78 (2002).
[24] A. Jablonski,, Surface Sci. **586**, 115 – 128 (2005).
[25] A. Jablonski, in Proceedings of the 4th International Conference on Solid Surfaces and the 3rd European Conference on Surface Science, Cannes, 1980, edited by D. A. Degras and M. Costa, Societe Francaise du Vide, Supplement a la Revue "Le Vide, les Couches Minces" no. 201, Paris, 1980.
[26] J. Cazaux, Microsc. Microanal. Microstruct. **4**, 271 (1992).